NUMERICAL STUDY OF MARANGONI COVECTION AND MASS TRANSPORT IN MICRODROPLETS

by

VIRAJ PARAG SABANE

Presented to the Faculty of the Graduate School of

The University of Texas at Arlington in Partial Fulfillment

of the Requirements

for the Degree of

MASTER OF SCIENCE IN MECHANICAL ENGINEERING

THE UNIVERSITY OF TEXAS AT ARLINGTON

MAY 2017

Acknowledgements

I dedicate this thesis to my parents. I am eternally thankful to my mother for her love, support and for extraordinary sacrifices she made. I am grateful to my father for his immense support and faith in me and my grandparents for being a great inspiration.

I would like to express my deepest gratitude to my advisor Dr. Moon for providing me with a research opportunity. I am thankful to her for her support, guidance and more importantly for the inspiration she continues to be.

I would like to extend my gratitude to Dr. Vinay Abhyankar and Dr. Miguel Amaya for being a part of my thesis defense committee.

A special thanks to MunMun Nahar for helping me learn and execute Comsol Multiphysics. Her insights were very helpful for me to overcome many challenges I came across in this research. I thank Ali Farzbod, Arvind Venkatesan, Shubodeep Paul for mentoring me throughout this research. I am also grateful to Ajinkya Shetye for helping me with experiments.

I thank Matin Torabinia for his support and encouragement throughout this research journey.

I am thankful to my roommates Sahil Raina and Souvik Dubey for their support throughout this journey.

April 25, 2017

Abstract

NUMERICAL STUDY OF MARANGONI CONVECTION AND MASS TRANSPORT IN MICRODROPLETS

Viraj Parag Sabane, MS

The University of Texas at Arlington, 2017

Supervising Professor: Hyejin Moon

Marangoni convection is a flow resulting from a surface tension gradient at air/liquid interface caused by temperature gradient, concentration of surfactant or applied electric field. Marangoni convection when caused by temperature gradient is also known as thermo-capillary effect. A micro gravity condition presents an ideal case to study this phenomenon since interfacial forces are dominant over body forces. Hence Marangoni convection inside a droplet squeezed between parallel plates was studied both numerically and experimentally. The potential application of Marangoni convection at microscale includes particle separation, chaotic mixing inside the droplet and possible enhancement in liquid-liquid extraction. To explore these applications, firstly flow field inside a droplet was studied by imposing variety of surface tension gradient. Secondly a comparative numerical study of mixing inside the droplet was done for pure diffusive and convective diffusive mixing cases, to evaluate the efficiency of Marangoni convection in mixing. Next, a biphasic system of an oil droplet rising in aqueous media was modelled to study effect of convection in liquid-liquid extraction. Finally, a biphasic system to study effect of Marangoni convection on liquid-liquid extraction was modelled.

Table of Contents

List of Illustrations

List of Tables

Chapter 1

Introduction to Marangoni convection

1.1 Marangoni convection

Marangoni convection is an interfacial phenomenon driven by surface tension gradient. Surface tension gradient can primarily have three causes, temperature gradient, concentration of solute and electric field. A general formulation uniting all three source is what follows [1].

$$\partial\gamma = \frac{\partial\gamma}{\partial T}\partial T + \frac{\partial\gamma}{\partial E}\partial E + \frac{\partial\gamma}{\partial C}\partial C$$

Where C, E, T, γ are concentration, electric filed, temperature and surface tension respectively. In this research work we focused on contribution of temperature gradient alone. Driving mechanism of Marangoni convection caused by temperature gradient can be explained with the of following figure.

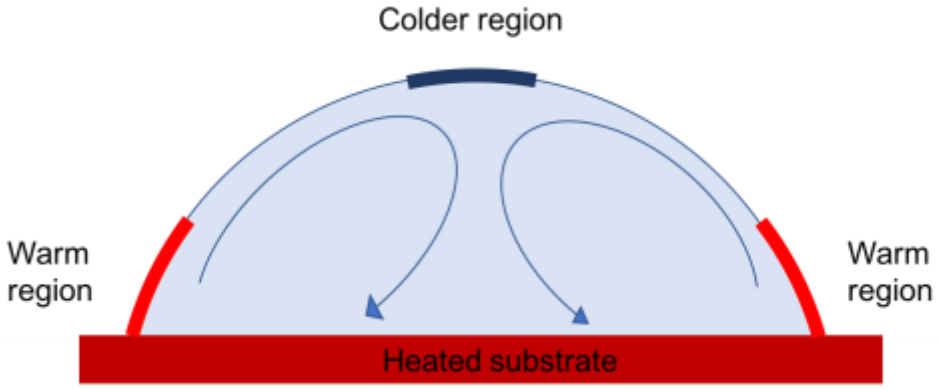

Figure 1 Sessile drop resting on a heated substrate

Figure 1 depicts a sessile droplet resting on a heated substrate. Naturally bottom portion of a droplet is relatively at higher temperature than that of the apex. Warmer region is also a region of lower surface tension and colder region is a region of higher surface tension, since the surface tension is inversely proportional to temperature. Due to this gradient in surface tension, an unbalanced force distribution is created at the interface,

where tangential force dominates viscous force. This unbalance of force creates a shear stress at interface which results in fluid motion along the interface. In other words, a tangential stress at interface yields a shear stress which transmits through viscous traction or fluid motion inside the droplet.

Hence the higher surface tension fluid at the apex pulls a bottom region fluid with lower surface tension along the interface and is recirculated back giving rise to Marangoni convection. This convection is strongest at the interface.

1.2 Microgravity condition

Since Marangoni convection is driven by temperature gradient, it is necessary to address the contribution of natural or thermal buoyant convection. There are two possible mechanisms driving internal flow in a droplet, first one being Marangoni convection second being buoyant convection. Marangoni convection is independent of gravity however at macro gravity condition it is masked by thermal buoyant convection. [2]

There is a simple criterion to eliminate the possibility of buoyant convection contribution to the internal flow. Bond number determines the strength of Marangoni and buoyant convection. Bond number is a ratio of Rayleigh number which determines strength of natural convection to Marangoni number which determines strength of Marangoni convection.

$$Bo = \frac{\alpha \rho g H^2}{\sigma_T}$$

$\alpha, \rho, g, H, \sigma_T$ are coefficient of thermal expansion, density, gravity, height or radius of a droplet, temperature derivative of surface tension respectively. For a bond number, less than one, buoyant convection can be neglected. [3]

Chapter 2

Numerical Study

2.1 Introduction

A finite element analysis software Comsol Multiphysics was used to numerically model a case of Marangoni convection to study the flow field. Finite element analysis is method to approximate partial differential equation(PDEs) numerically. The physics for most time and space dependent problem are expressed in terms of partial differential equations, often these PDEs cannot be solved analytically. A commercial software such as Comsol approximates these PDEs with numerical model equations and solution of which are obtained by numerical methods. [4]

2.2 Modeling

A single-phase 3D model was constructed. Three cases of Marangoni convection in sandwich droplet with variations in applied temperature gradient were studied. Variations in temperature gradient were modelled by changing heater shape and positioning. Modeling involves total of four step. First is building a geometry which is consistent with a real system, second is selecting and coupling right physics, next step is meshing where system is discretized in numerous small element, finally the solution is obtained by solving PDEs for each of the discretized element.

2.3 Assumptions

Following were the assumptions made for mathematical description of the system:

1. Temperature has no effect on viscosity of the liquid droplet and air, i.e. fluid is Newtonian.
2. The liquid and surrounding air is incompressible.

3. Internal fluid flow does not deform the droplet, which is a reasonable assumption for low bond number.
4. Liquid droplet does not evaporate.
5. Shape of the sandwiched droplet is cylindrical.

2.4 Governing equations

Marangoni convection is modelled using two physics, first one being single phase laminar flow and second one being heat transfer in fluids. Moreover, these two physics must be coupled both ways since both velocity field and temperature field are interdependent, meaning a convection is set in due to temperature gradient and at the same time convection changes the temperature profile. To obtain solution for such a system, following set of equations are required to be solved.

To obtain a solution for flow field, incompressible Navier-Stokes equation is solved along with continuity equation. The solution to these equations yields velocity field and pressure distribution.

$$\rho(\frac{\partial u}{\partial T} + u \cdot \nabla u) = -\nabla \mathrm{p} + \nabla \cdot (\mu(\nabla \mathrm{u} + (\nabla u)^T) + F$$

$$\nabla \cdot (\rho u) = 0$$

Navier-stokes equation represents conservation of momentum while continuity equation represents conservation of mass.

To obtain a solution for temperature field, energy equations are used.

$$\rho C_p \frac{\partial T}{\partial t} + \rho C_p u \cdot \nabla T + \nabla \cdot q = Q + Q_p + Q_{vd}$$

$$q = -k \nabla T$$

The convective heat transfer depends on velocities from momentum balance, thus a coupled system is solved using non-linear solver.

2.5 Multiphysics coupling

Two multiphyics coupling were used, one incorporates dependence of convective heat transfer on the velocity in momentum balance, second relates the shear stress at free surface to the surface tension gradient.

The Boussineq approximation, an expression that includes temperature and acts as a force in y-direction in momentum balance, is used to couple velocity field and temperature field. [5]

To model maragoni effect, it is essential to couple shear stress and temperature gradient, since the induced shear stress at interface is a driving mechanism behind convection. Following is the equation which couples shear stress with temperature gradient. [6]

$$\eta \frac{\partial u}{\partial y} = \gamma \frac{\partial T}{\partial x}$$

Thus a shear stress term in Naveir Stokes equation is equated with a tangential stress term, the tangential component of shear stress at interface must balance tangential stress arising from gradient in surface tension.

$$\nabla \cdot (\mu(\nabla u + (\nabla u)^T) = \gamma \nabla_t T$$

2.6 Models

Imposing a temperature gradient yeilds a surface tension gradient at the interface and is responsible for internal convection inside the droplet, we studied this convection under various temperature gradient conditions. A total of three models were built, each having different kind of imposed temperature gradient. All three models shows, how an internal flow can be engineered by using various heating schemes.

2.6.1 Type I: Bottom and top heater

Model as shown in Figure 2(a) consists of six domains. Table 1 enlists domain material.

Table 1 Materials

Domain	Material
Top chip	Silica glass
Bottom chip	Silica glass
Top heater	Indium tin oxide
Bottom heater	Indium tin oxide
Droplet	Ionic liquid
Gap	Air

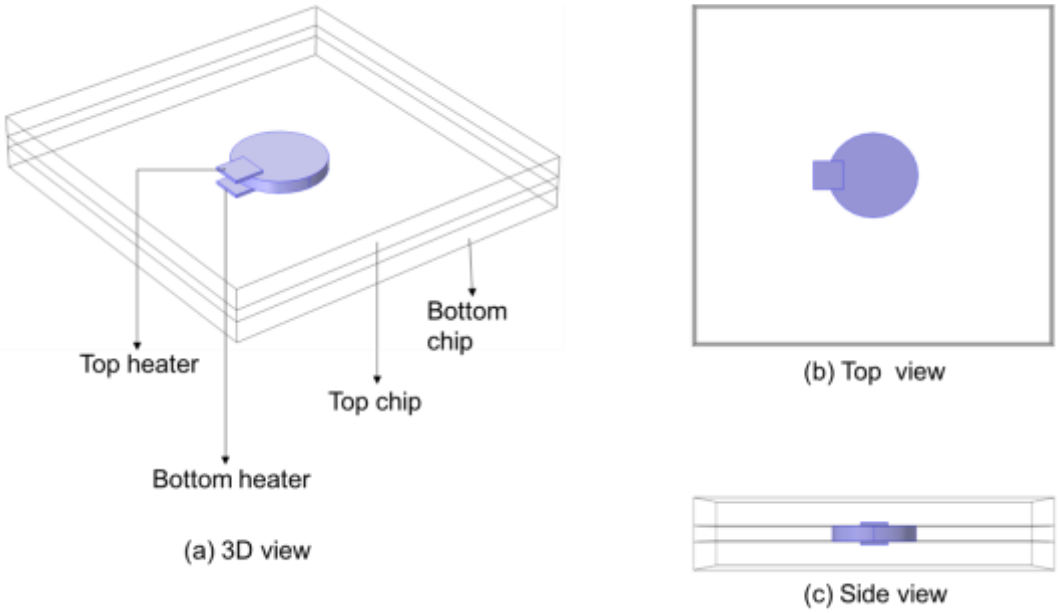

Figure 2 Model geometry: (a) 3D, (b) top and (c) side view.

Table 2 lists dimensions of the model.

Table 2 Dimensions of the model

Domain	Length (mm)	Breadth (mm)	Height (mm)
Top chip	12	12	0.7
Bottom chip	12	12	0.7
Gap	12	12	0.4
Heater	1	1	0.1

Droplet	Diameter (mm)	Height (mm)
	3	0.4

2.6.1.1 Initial conditions

Zero initial velocity, atmospheric pressure and temperature of 298 K are considered.

2.6.1.2 Boundary conditions

For the laminar flow interface, a slip condition is imposed on free meniscus and a no slip condition is imposed on top and bottom surfaces.

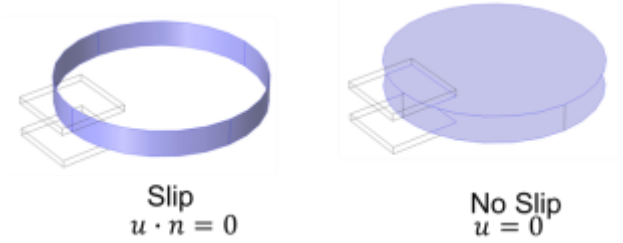

Figure 3 Boundary condition for fluid flow interface.

A slip boundary condition is a no penetration condition, a velocity normal to the boundary is set to zero so that fluid does not exit from the boundary. A no slip boundary condition sets velocity at the boundary as zero.

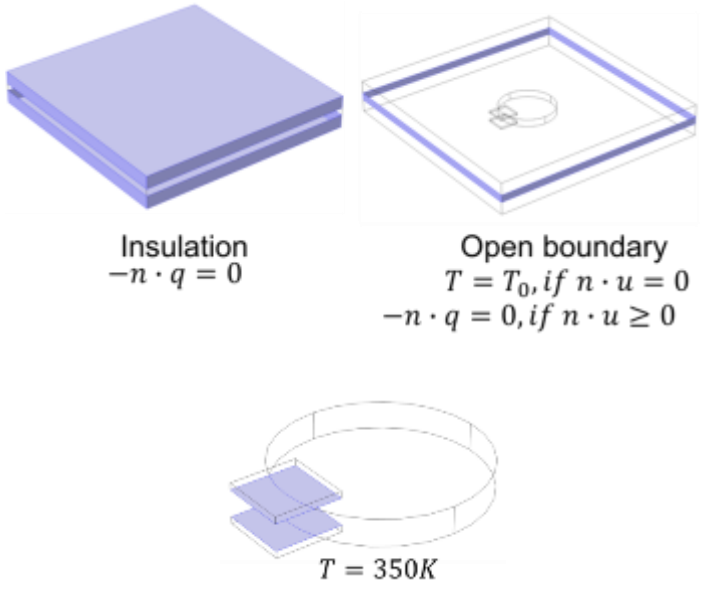

Figure 4 Boundary conditions for heat transfer interface.

For the heat transfer interface, a boundary condition of insulation is imposed on top and bottom plate, where as an open boundary condition is defined at the boundary of air domain. Moreover the boundary of heater which is in contact with liquid is set to 350 K.

2.6.1.3 Meshing

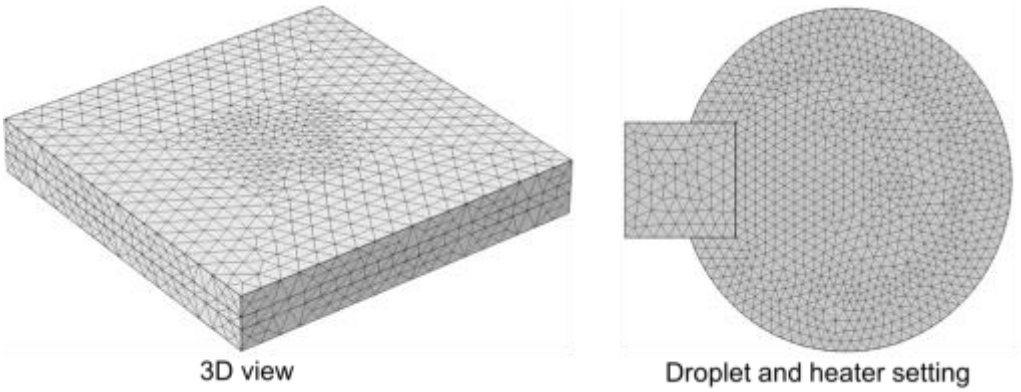

Figure 5 Finer mesh.

Process of discretization of geometry in numerous smaller element is known as meshing. PDEs are solved for each of such element and an approximate solution is obtained. A finer mesh with total 126329 elements was used in this case as shown in Figure 5.

2.6.1.4 Solution

A non linear time dependent solver is used to obtain a solution. Solution to Navier stokes equation gives velocity and pressure field, whereas solution to energy equation gives temperature field.

2.6.1.5 Results

Once a solution is computed, a velocity and temperature profile is plotted. It was evident from the temperature profile that temperature gradient exists in xy plane. No temperature gradient in zx or zy plane, due to symmetric positioning of the heater. Temperature profile is as follows.

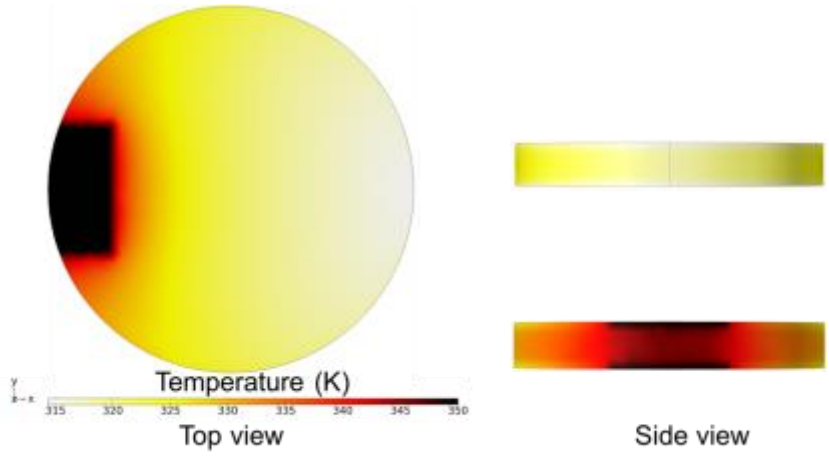

Figure 6 Temperature profile of a droplet

Since surface tension is inversely proportional to temperature, the region of high temperature is also a region of low surface tension and region of low temperature is also a region of high surface tension.

As observed from the following velocity profile, fluid travels from region of low surface tension to region of high surface tension along the meniscus and is recirculated back forming two symmetrical vortices in yz plane, also no fluid motion is observed in z plane. A maximum velocity is observed at the interface.

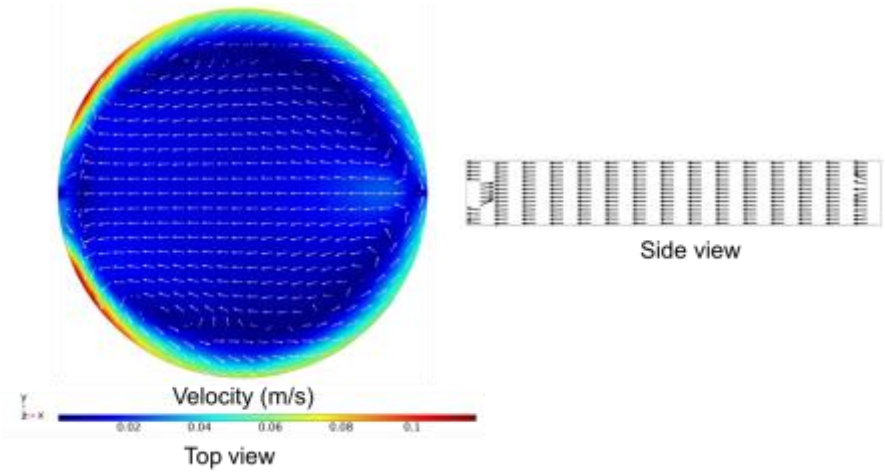

Figure 7 Velocity profile of the droplet.

2.6.2 Type 2: Linear heater

A second variation in temperature gradient is imposed by using a lineat heater as shown in Figure 8 model. A linear heater is placed on top of the cylindrical droplet.

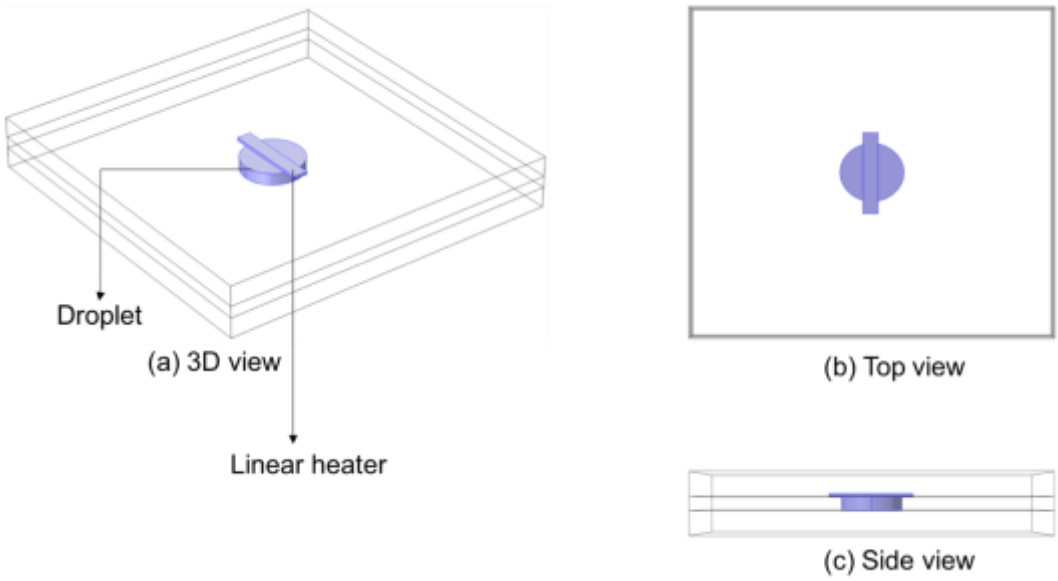

Figure 8 Model geometry (a) 3D, (b) top and (c) side view

Model in Figure 8(a) contains five domains; those are top chip, bottom chip, air gap, droplet and heater. Diamensions for all domains except for heater are same as that in the case of type I. The diamensions of linear heater are 3mm x 0.5mm x 0.1mm (lxbxh).

Similar to case of type I heater scheme, materials were assinged to each of the five domains.

2.6.2.1 Initial conditions

Initial velocity was set to zero, atmosperic pressure and temperature of 298 K were considered.

2.6.2.2 Boundary conditions

All boundary conditions were similar as in the case of type-I heater scheme, except for temperature condition at the boundary of heater and droplet, which was set to 400 K.

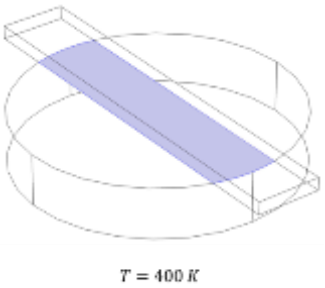

Figure 9 Boundary condition at heater-droplet interface.

2.6.2.3 Meshning

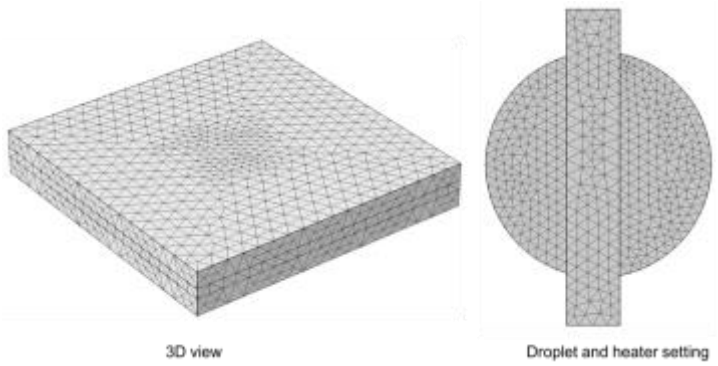

Figure 10 Mesh 3D view and magnified view of droplet and heater setting.

All domains were discretized in 103429 elements and a nonlinear solver was used to obtain the solution.

2.6.2.4 Results

A temperature profile and velocity profile are as shown in Figure 11 and 12, respectively. Temperature gradient was observed in xy plane and in z direction at two ends of the heater.

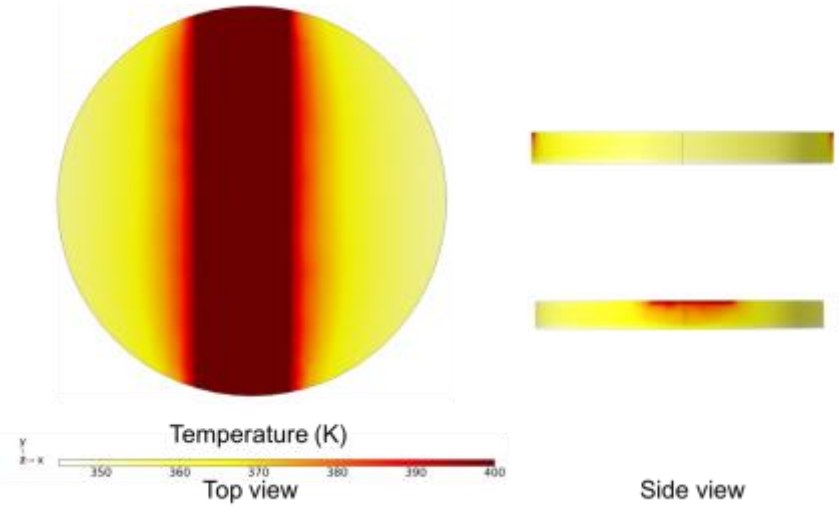

Figure 11 Temperature profile of a droplet

Following is a velocity profile,

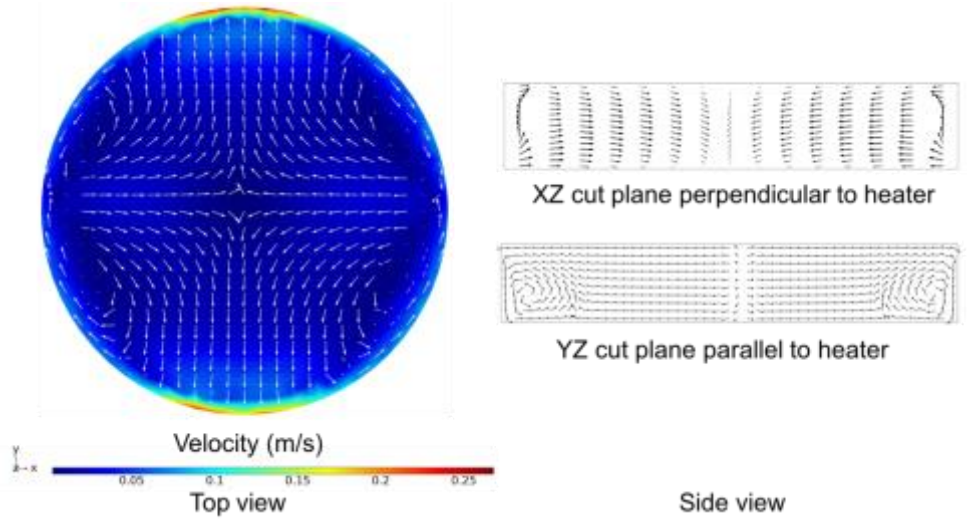

Figure 12 Velocity profile: top view and side view.

As seen from the velocity profile, fluid travels from high temperature region (low surface tension region) to low temperature region (high surface tension region) along the meniscus and is recirculated back forming four symmetric vortices. Maximum velocity was observed at meniscus.

2.6.3 Type 3: Ring heater

A third variation to temperature gradient is imposed by ring heater as shown in the following model. A ring heater is placed as such that it heates a portion of free surface.

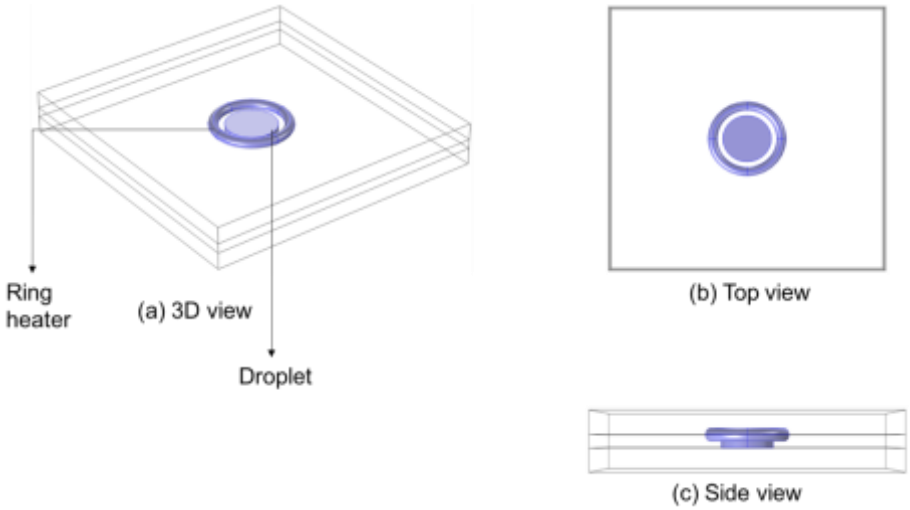

Figure 13 Model geometry (a) 3D, (b) top and (c) side view.

Model in Figure 13 (a) contains five domains; top chip, bottom chip, air gap, droplet and ring heater. Dimensions for all domains are same, except for ring heater. The center of ring heater aligns with the center of the droplet. Like in case of type 1 and 2 heater scheme, materials were assigned to each of the domain.

2.6.3.1 Initial condition

Initial velocity was set to zero, atmosperic pressure and room temperature of 298 K were considered.

2.6.3.2 Boundary conditions

All boundary conditions used in this model were similar, except for boundary temperature at the heater surface, which was set to 450 K as shown in Figure 14.

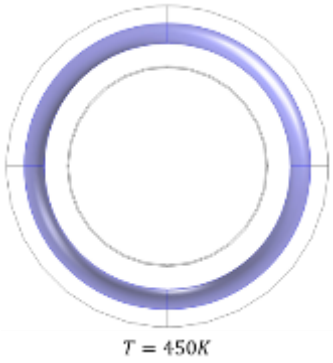

Figure 14 Temperature condition at heater boundary

2.6.3.3 Meshing

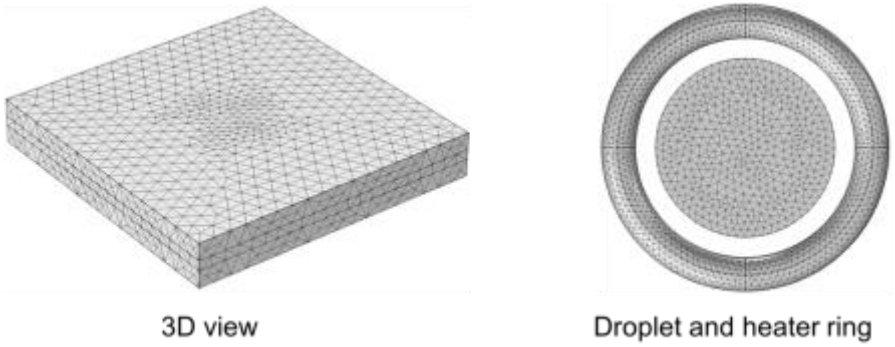

Figure 15 Mesh: 3D view and Droplet-heater setting.

Entire geometry was discretized in 149804 elements. Solution was obtained by solving PDEs for every element using a nonlinear solver.

2.6.3.4 Results

Temperature profile and velocity profile were plotted in Figure 16 and 17 respectively, temperature gradient is observed in z direction. No temperature gradient is observed in xy plane due to symmetric positioning of ring heater. Also the region of high temperature is a region of low surface tension and region of low temperature is a region of high surface tension. An interesting temperature profile is obtained. In the near region of free surface at both end of temperature profile plane, rolls can be observed, which indicates the effect of velocity field on temperature profile.

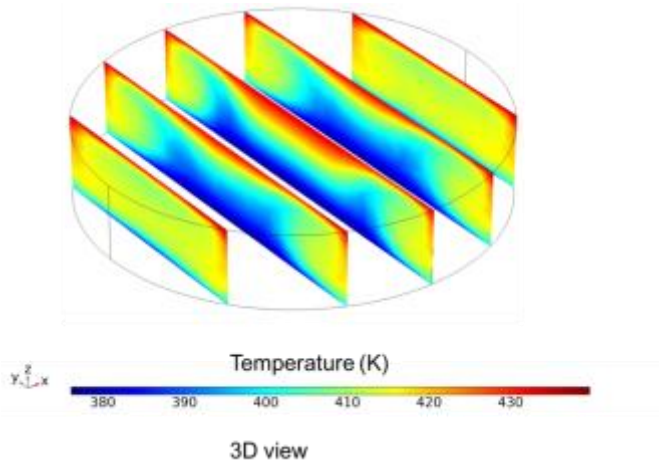

Figure 16 Temperature profile of the droplet.

Velocity profile obtained is as follows,

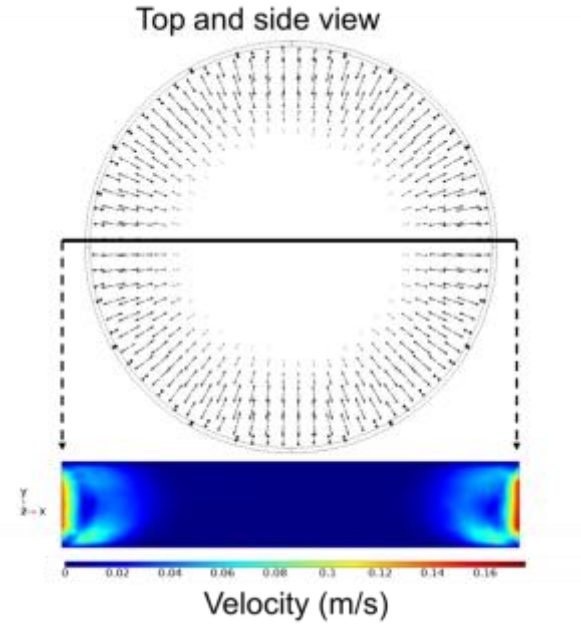

Figure 17 Velocity profile.

Fluid flow from top to bottom along the interface and is recirculated back forming convective rolls at the free surface, which is evident from the velocity profile plotted on a

cut plane (side view) in the Figure 17. The convection is limited to some radial distance from free surface, leaving the fluid at the center undisturbed. This kind of flow field has a potential application where fluid isolation is of the interest.

2.7 Summary

1. Internal flow in a droplet can be manipulated by using various heating schemes.
2. Velocity of a fluid flow is maximum at the meniscus.
3. At microscale, convection driven by thermal phenomenon is dominated by marangoni convection.

Moreover, possibility of using heater as a means to impose temperature gradient, in turn to impose surface tension gradient which generates marangoni convection have several advantages. As seen in previous chapter, Marangoni flow can be engineered by imposing variety of temperature gradient which is possible by changing heater geometry and placement. The ability to impose localized temperature gradient allows precise control and localization of flow.

Furthermore, Marangoni convection is proportional to applied temperature gradient. Greater the temperature gradient, higher is the fluid velocity. Thus faster velocities can be achieved by only small change in temperature by applying a sharp temperature gradient.

Ability to localize flow and prciese control over flow velocities can have several applications in micro pumps, micro mixers, actuators, etc. [7]

In this work we explored possible application of Marangoni convection in droplet based particle separation, droplet based chaotic mixing and enhancement in liquid-liquid extraction.

Chapter 3

Application I: Particle separation in a droplet

3.1 Introduction

Particle separation techniques have applications in biological and biomedical devices, one important example is cancer cell separation. In recent years, several particle separation techniques have been developed, some of the most popular techniques are based upon acoustics, optics and magnetism [8]. However, in this work, we focused on hydrodynamic aspect of particle separation.

3.2 Literature review

Response of particle to hydrodynamic forces is of critical importance to achieve particle separation. Particle in fluid flow experiences both hydrodynamic forces, shear stress parallel to flow direction and normal stress perpendicular to flow direction. Drag force accelerates particle in downstream direction and lift force acts perpendicular to this drag force. This lift force scales greatly with particle diameter, thus particle of different sizes has a response which scales differently and this fact is exploited in particle separation. [9] Di carlo group successfully separated particles by using a system of straight and curved microchannel. Separation was achieved in two steps. First step was equilibrium positioning. Equilibrium position refers to a stationary point of dynamical system. Equilibrium position is determined by balance of hydrodynamic forces acting on the particle.

Ho and Leal in their work explains following two component of lift force responsible for equilibrium positioning of a particle in a straight microchannel. [10]

1. Lift force by wall effect
2. Lift force by gradient in shear

Physics of equilibrium positioning can be explained with help of Figure 18,

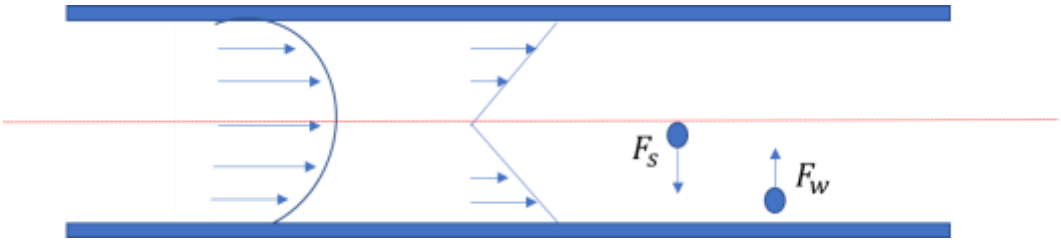

Figure 18 Schematic of lift forces acting on a particle.

F_s component of lift force pushes particle from channel center line towards the wall and is caused by gradient in shear which is evident from velocity and shear stress profile in above figure. F_w component of lift force pushes particle from wall towards channel center line and is caused by asymmetric wake at channel wall. Equilibrium position is determined by balance between these two components and more dominantly is determined by F_s component due to higher magnitude.

Once particle reaches an equilibrium position, it continues to maintain the same position unless an external force with a competitive magnitude acts on the particle to displace it. Also, the equilibrium position is independent of particle size, therefore a spectrum of micro particle will assume the same equilibrium position, only length of channel required to migrate to equilibrium position will differ. [11]

Equilibrium position is located at some distance from the channel wall and is also dependent on channel geometry. Equilibrium position for a square micro channel is as shown in Figure 19.

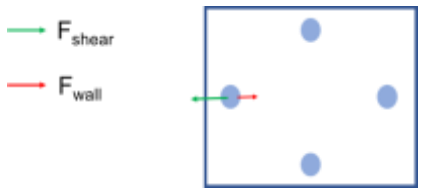

Figure 19 Equilibrium position of particle in a square micro channel.

For a square channel, there are four symmetric equilibrium positions, however these four position can be reduced to single point by engineering the channel geometry. [11]

They also experimentally determined the independence of equilibrium position on density of particles. However, it is important to mention that equilibrium positioning cannot be achieved for neutrally buoyant particles i.e. for particles having same density of the fluid which it is suspended in.

Second stage of particle separation is equilibrium separation. Once particles reach equilibrium position in straight micro channel, the fluid is passed through a curved micro channel, as shown in Figure 20.

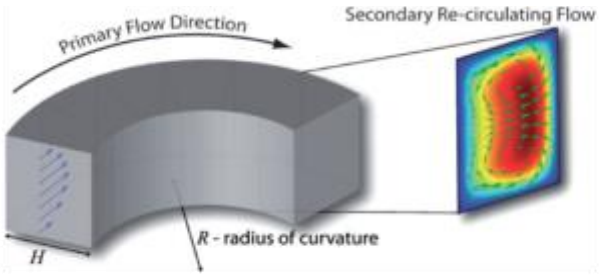

Figure 20 Fluid flow through curved microchannel [10]

A fluid passing through a curved microchannel still have a parabolic profile i.e. there is gradient in velocity at channel center line and near wall region, thus fluid at channel center line have a greater inertia than fluid at channel wall region. Hence fluid at channel center line flows outward and is recirculated back giving rise to secondary re-circulating flow as seen in above figure. Thus, primary flow and secondary flow acts in superposition and are orthogonal to each other. Secondary flow is also known as Dean's flow.

Thus, an additional drag force due to secondary flow acts on particle, in superposition with hydrodynamic forces of primary flow. Deans drag force acts to entrain particles in secondary recirculating vortex displacing them from pre-assumed equilibrium position.

However, dean's drag force selectively affect particles, depending on their size. This phenomenon can be explained with help of Figure 21,

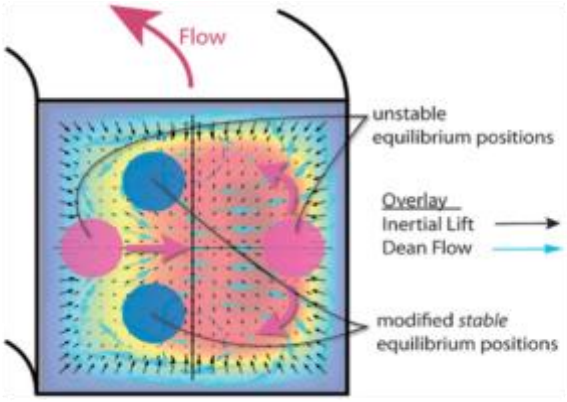

Figure 21 Particle separation [10]

Particle held stationary at equilibrium position will experience dean's drag force which is proportional to local velocity of secondary vortex and is perpendicular to direction of primary flow.

Particles response to a dean's drag force depends on its size, such that smaller particles are entrained in secondary dean's vortex, particle of intermediate size are displaced to modified equilibrium position and larger particle maintains their initial equilibrium position. As seen from Figure 21, particles are displaced to modified equilibrium position since deans drag force destabilized initial equilibrium position.

The important conclusion from literature survey is that once particle assumes equilibrium position, the separation is possible only when an additional force acts on a particle which can compete with hydrodynamic forces responsible for maintaining the equilibrium position. [12]

Next, we performed an experiment to explore possibility of droplet based particle separation by using Marangoni convection.

3.3.1 Experiment details

The aim of the experiment was to analysis particle trajectory in a Marangoni flow. Figure 22 is the schematic of experimental setup,

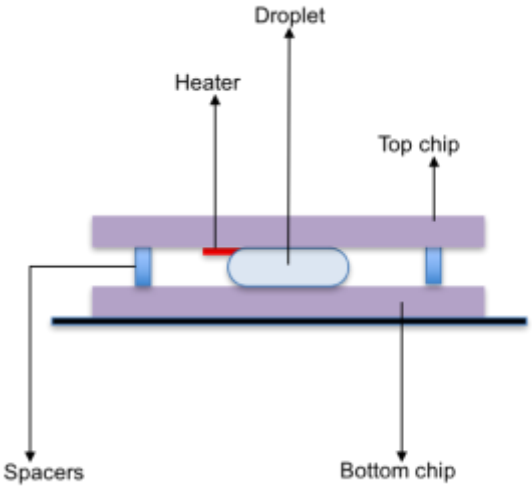

Figure 22 schematic of the experimental setup (side view)

Table 3 enlists material of each of apparatus,

Table 3 Materials and apparatus

Apparatus	Material
Bottom and Top chip	Silica glass
Droplet	Ionic liquid
Spacers	Kapton tape
Heater	ITO heater

A droplet is sandwiched between top and bottom chip, which are separated by two spacers. Bottom chip have a hydrophilic opening to keep droplet in one place and top chip have an ITO heater, heater patterned on top chip is used to heat the droplet. Thickness of bottom and top chip is 0.7 mm and spacer thickness 0.18 mm. Overall setup is as represented in Figure 22. What follows is the magnified view of actual experimental setup of droplet sandwiched by top and bottom chip (Figure 23).

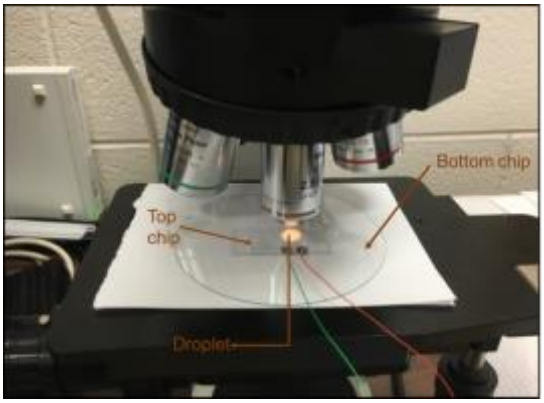

Figure 23 Magnified view of the experimental setup

The ITO heater on top chip is connected to power source by using 30-gauge wire. To make this connection, copper strips are attached to contact pads of ITO heater by using a silver epoxy, then wires are soldered on the copper strip. Overall setup is as seen in figure 24,

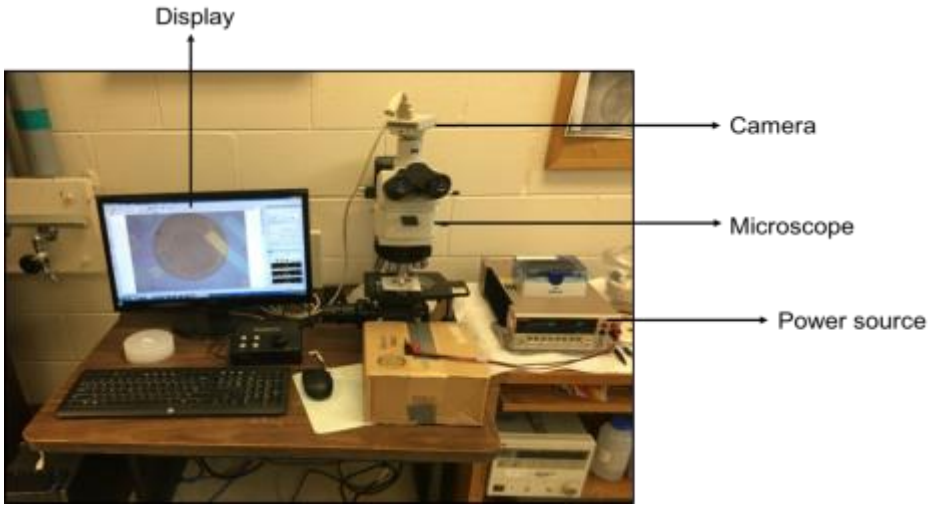

Figure 24 Overall setup

Internal flow in a droplet was observed and recorded using a Nikon LV 150 microscope which have an integrated camera.

3.3.2 Experiment procedure

First step was to suspend nylon particles of size 40 μm in ionic liquid, it was done by thoroughly mixing the ionic liquid and nylon particles by using a vortex mixture followed by sonicating. Ionic liquid (C34H68F6NO4PS2) was used as a working fluid to suppress evaporation. ITO heater was connected to power source to supply current. An ionic liquid drop of volume 2 μl mixed with nylon particles was dispensed on bottom chip at hydrophilic opening. Spacers are then placed on bottom chip such that a gap of 400 μm can be maintained. Droplet was then sandwiched by carefully placing the top chip on spacers. Fine adjustments are made while placing a top chip such that ITO heater is in contact with droplet meniscus as shown in 25(b),

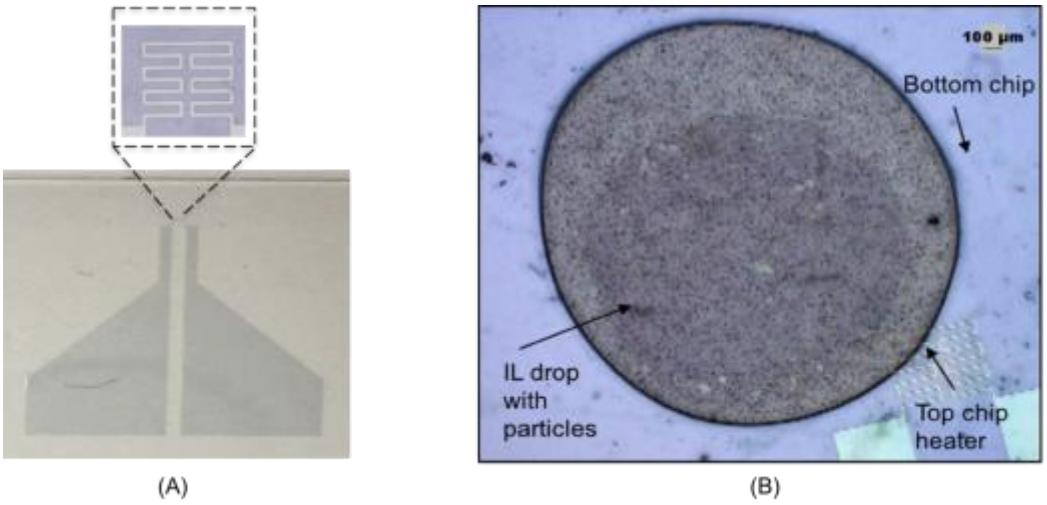

Figure 25 (A) magnified view of ITO heater, (B) Heater placement on droplet

A current of 12 mA is then passed through a heater whose resistance is 1523 Ω, which produced a heat flux of 87.72 w/cm^2. Thus, temperature in region near heater was more and in region away from the heater was less. Due to this gradient in temperature, a surface tension gradient was produced and in turn Marangoni convection was generated. Results and conclusion are as discussed in following section.

3.3.3 Observations

Figure 26 shows that flow field resulted in,

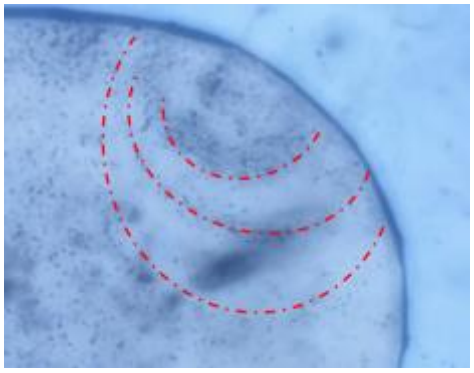

Figure 26 Flow field

On careful analysis of the video, a repetitive pattern of particle trajectory over a long period (26 minutes) was observed. A recirculating flow forming a vortex was seen. Three distinct streamlines were observed and particle entrained in respective stream line stayed in the same streamline, this can be attributed to the fact that at micro gravity condition for a low Reynold number flow, the inertial forces are negligible. Thus, we concluded that the particles have assumed an equilibrium position and Marangoni convection alone will not suffice to achieve particle separation.

In this case, particle separation can be achieved by selectively displacing particle from their equilibrium position. Thus, an additional force with magnitude that can compete with Marangoni convection is required. The magnitude should be as such that it selectively displaces particle depending on their size.

Possible means to introduce an additional force can be, droplet movement or wetting and dewetting. Next section addresses the summary for particle separation theory and experiment.

3.4 Summary

Following are the important conclusions from particle separation theory,

1. Particle trajectories are greatly influenced by hydrodynamic forces acting on the particle.
2. Due to small size of droplet, the effect of gravity is negligible.
3. Particle does not have any effect on the flow field.
4. For a low Reynold number flow or creeping flow, particle once entrained in a streamline, continues to stay in same streamline unless an additional force is introduced.

Moreover, hydrodynamic forces scale greatly with size and shape of the particle, combining this fact with micro gravity condition where effect of gravity is negligible, we concluded that particle trajectory at microscale is function of particle shape and size only.

What follows are the conclusion from experiment on particle separation by Marangoni convection,

1. On careful observation of Marangoni convection inside the droplet, three distinct streamline were observed.
2. Maximum velocity was observed at the free surface.
3. Particle assumed equilibrium position in the given stream line i.e. particle once entrained in a stream line, stayed in a same streamline.

Thus, to achieve particle separation with only Marangoni convection was not possible. We concluded that, to achieve particle separation, an additional force must be introduced such that it can displace particle from their equilibrium position.

Chapter 4

Application II: Chaotic mixing in a droplet

4.1 Introduction

Mixing at microscale is one of the important aspect of microscale analysis systems, since miniaturizing brings advantages to field such as chemical industry, pharmaceutical industry, biochemical and biomedical analysis. However, mixing at micro scale have its own challenges, for example, turbulent mixing at macro scale is not possible in microscale due to the laminar and deterministic nature of flow caused by dominant viscous effects. Moreover, molecular diffusion is slow process, thus requires greater length scale for mixing. [13]

Moreover, convection have proven to enhance mixing, thus we investigated chaotic mixing inside a droplet. Mixing dynamics in a droplet was studied by simulating the system in Comsol Multiphysics. The goal of a numerical simulation was to study how Marangoni convection enhances mixing inside a micro droplet.

4.2 Numerical study

A model for sessile droplet was created, to study efficiency of Marangoni convection to enhance mixing. Initially a vertical concentration was assumed such that all the solute was in lower half of the droplet as shown in Figure 27,

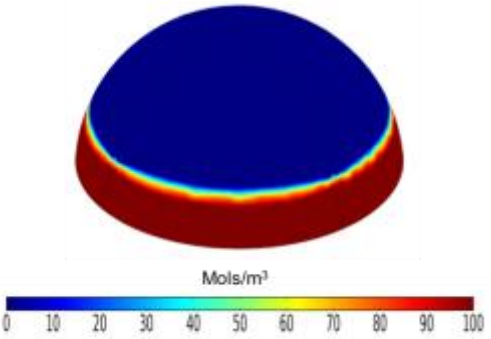

Figure 27 Initial concentration condition of a sessile droplet

To obtain solution for this system, total of three physics namely laminar flow, heat transfer and transport of diluted species were coupled and solved. Firstly, Marangoni convection was modelled. Flow field and temperature profiles were obtained by solving equations of momentum balance and energy balance, respectively.

The flow field obtained from momentum balance equation is then used in following convective diffusion equation to account for mass transport,

$$\frac{\partial c}{\partial t} + u \cdot \nabla c = \nabla \cdot (D \nabla c) + R$$

Boundary conditions for heat transfer interface was such that the temperature of bottom surface of droplet was maintained at 450 K. Thus, a temperature gradient was generated on the droplet free surface. Due to applied temperature gradient, a surface tension gradient was generated and in turn tangential stress was generated on the droplet meniscus. To balance this tangential stress a recirculating flow was generated along the meniscus such that fluid flows from bottom to top and is recirculated back.

Note that results in figure 29, 30 and 31 are plotted on cult plane as shown in Figure 28.

Figure 28 Cut plane

Figure 29 and 30 are the temperature and velocity profile, respectively.

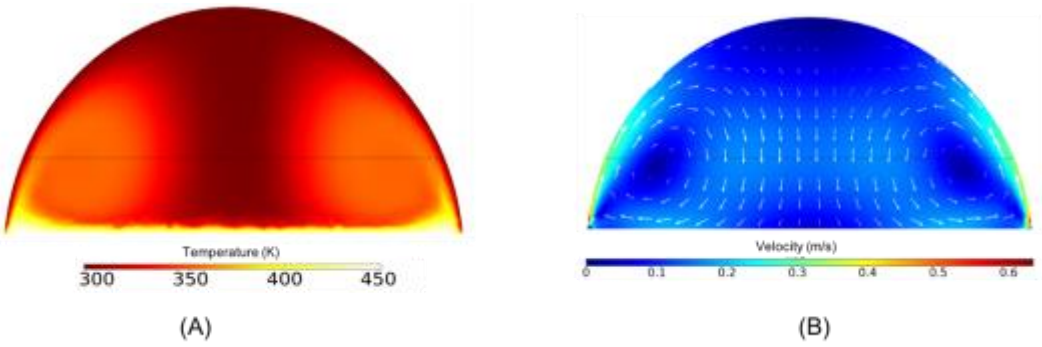

Figure 29 (A) Temperature profile, (B) Velocity profile

It can be seen from figure 29(a), that a temperature gradient exists in the vertical direction, bottom surface of a droplet is at higher temperature whereas top portion is at lower temperature. As seen from the velocity profile in figure 29(b), the fluid travels from bottom to top along the meniscus and is recirculated back forming two symmetric vortices in the plane. Also, the velocity at the meniscus is highest.

Concentration profile is as shown in the Figure 30.

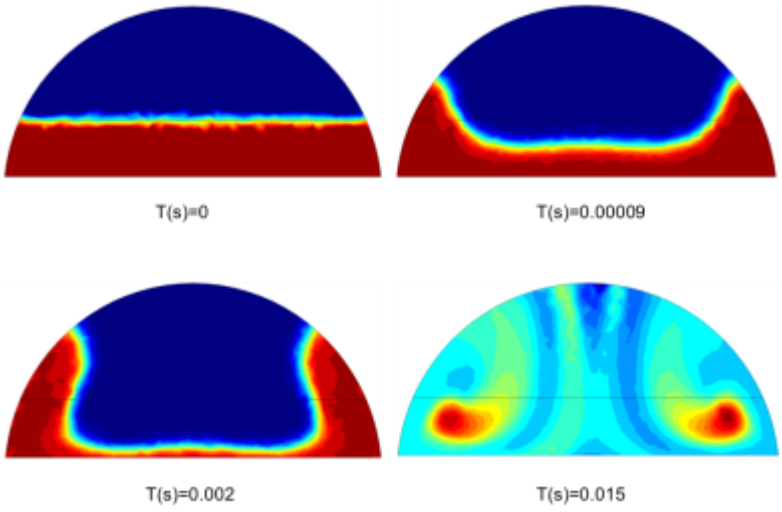

Figure 30 concentration profiles

Figure 30 demonstrates convective diffusive mixing, initially solute is concentrated in the lower half. When the internal flow or Marangoni convection is generated, the solute is mixed inside the droplet, making concentration homogeneous. Convective mixing dominates over the diffusive mixing, since the diffusion is a very slow process. Figure 31 shows mixing by pure diffusion for same time frame,

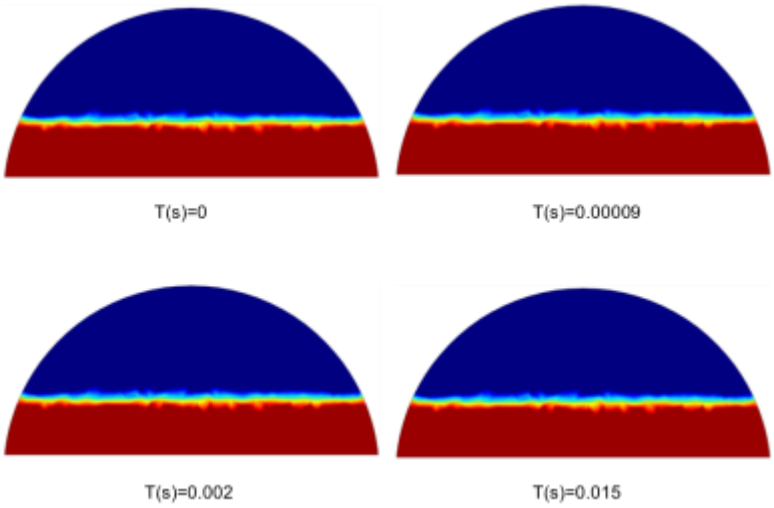

Figure 31 Pure diffusive mixing

It is evident from Figures 30 and 31, that diffusive mixing is very slow and it does not have significant contribution when mixing is promoted by convection.

4.3 Summary

Following are the conclusions from the numerical study,

1. Mixing inside the droplet is greatly enhanced by internal circulation.
2. Mixing pattern observed are consistent with the law that mass transport inside the droplet is done by symmetric vortices while stretching and folding as described by Baker's transformation.

Next chapter address effect of convection on liquid-liquid extraction.

Chapter 5

Application III: Enhancement in liquid-liquid extraction in microdroplets

5.1 Introduction

Liquid-liquid extraction is a technique to separate compounds based on their solubility in two different immiscible liquid. Liquid-liquid extraction is of a vital importance in field such as chemical industries, bio chemical analysis and radiochemical reaction. Liquid-liquid extraction at macro scale poses disadvantages such as high requirement of chemical and solvents. However microfluidic technology has several advantages such as high surface to volume ratio, ability to control flow accurately and reduced chemical quantities. The most important advantage of using microfluidic techniques is high surface to volume ratio, since mass transport in liquid-liquid extraction essentially takes place through interface between two liquids. In this work, we explored possibility of using Marangoni convection to enhance liquid-liquid extraction.

5.2 Literature review

Liquid-liquid extraction can be explained with help of Figure 32,

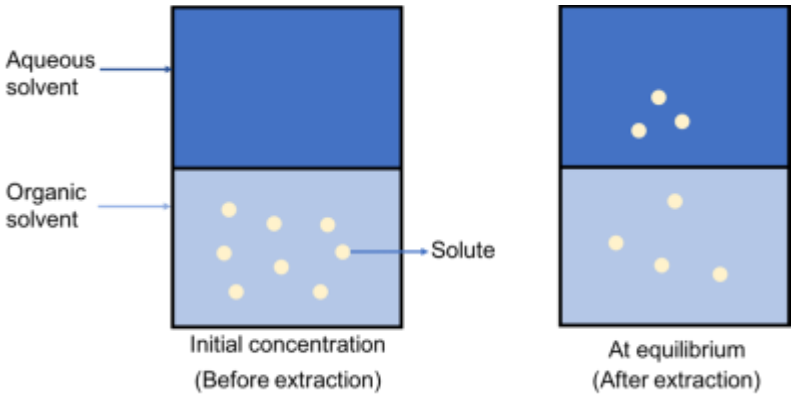

Figure 32 Liquid-liquid extraction

As shown in figure 32, aqueous and organic phase are in contact with each other. Initially all the solute is concentrated in the organic phase and hence there is a concentration gradient. Due to concentration gradient, solute is transported from the organic phase to

the aqueous phase. This mass transfer occurs across the interface between two phases, it is a non-equilibrium process characterized by motion of solute down the concentration gradient. [14]

It is important to note that transport of solute stops at equilibrium and often concentration in both phases are not equal at equilibrium. The amount of solute transported is limited by the partition coefficient which is a ratio of solubility in one phase to the other. Equilibrium condition and partition coefficient can be explained with figure 33,

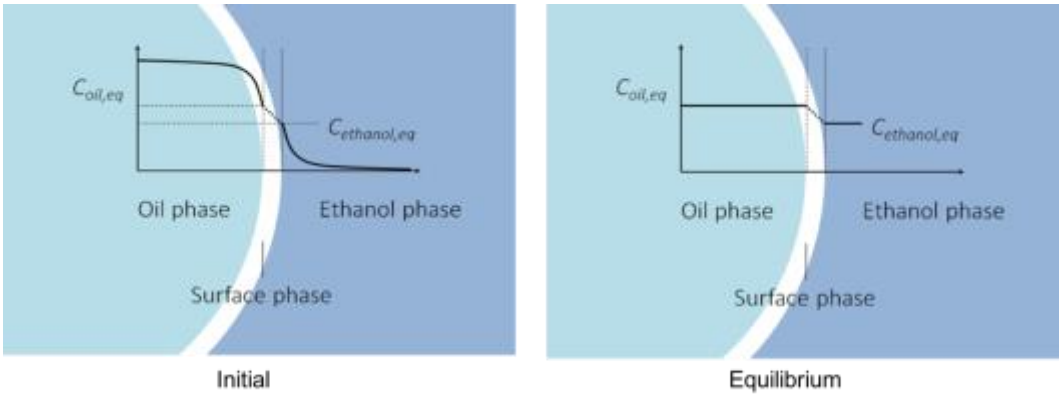

Figure 33 Concentration at initial condition and equilibrium [15]

In Figure 33, oil and ethanol phases are in contact. The interface between two phases is treated as the surface phase which contains molecules of both oil and ethanol. Initially all solute is concentrated in the oil phase. Due to concentration gradient, solute is transported from the oil phase to the ethanol phase and mass transfer rate is very low. Concentration in surface phase or an interface is at equilibrium since mass transfer rate in this phase is very high. At equilibrium, the mass transport stops and the amount of solute transported is governed by partition coefficient given by following equation,

$$K = \frac{C_{oil}}{C_{ethanol}}$$

where K is partition coefficient, C_{oil} is concentration in oil phase, $C_{ethanol}$ is concentration in ethanol phase.

It is important to note that concentration in both phases at equilibrium are not equal but depends on solubility in respective phase. Moreover, liquid-liquid extraction is a slow process. Furthermore, the convection has known to enhance extraction efficiency. Thus, we performed a numerical simulation to study effect of convection on liquid-liquid extraction as addressed in next section.

5.3 Numerical study

A two-phase numerical simulation was done on comsol to study effect of Marangoni convection on mass transfer rate. However, model incorporating Marangoni convection and convective mixing is a very complex problem. Thus, a simple two phase system of oil droplet rising in aqueous solution was modelled.

Before explaining the numerical model, it is important to address a level set method used to model a biphasic fluid system.

5.3.1 Level set method

Numerical modelling of a multiphase flow is often difficult because of difficulty in tracking a fluid fluid interface and a steep jump in fluid properties such as density and viscosity. A level set method which is based on continuum approach is used. Strength of this method lies in its ability to tack the interface [16]. This method uses a smooth function named levels set function ϕ, which is used to define a boundary between two immiscible fluids. Level set method can be better explained with help of Figure 34.

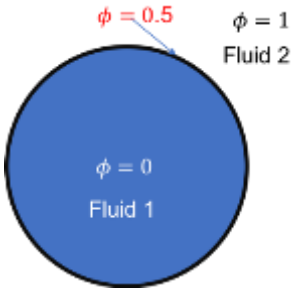

Figure 34 Schematic of a biphasic fluid system

In a biphasic system, value of level set function is set to zero for one fluid and its value is set to one for the second fluid, so that the level set function maintains value of 0.5 at the interface.

The interface movement is captured by following advection equation,

$$\frac{\partial \phi}{\partial t} + \nabla \cdot (\phi \vec{u}) = \gamma \nabla(-\phi(1-\phi)\frac{\nabla \phi}{|\nabla \phi|} + \varepsilon \nabla \phi)$$

Here γ is an initialization parameter and ε is an interface control parameter. This equation is solved with momentum balance equation. The suitable value for γ is maximum velocity of flow in the model. ε is an interface control parameter which determines the thickness of an interface, since that interface is very thin, ε should have a very small value, Comsol Multiphysics by default sets this value to half of the maximum length of mesh element.

Moreover, the densities and viscosities of both fluids are different. To introduce a smooth variation of these propertied following equations are used, [17]

$$\rho = \rho_1 + (\rho_2 - \rho_1)\phi$$

$$\eta = \eta_1 + (\eta_2 - \eta_2)\phi$$

Where ρ is density and η is viscosity of the fluid, subscript 1 and 2 represents respective fluid as shown in Figure 34.

Next section addresses numerical model of liquid-liquid extraction.

5.3.2 Model

A two-phase model of oil droplet rising in an aqueous phase was created, goal of this model was to study effect of convection on interfacial solute transport from a droplet to aqueous phase. Due to simplicity of this model, the computational time required was low. This allowed us to perform a parametric study, same was the motivation behind using this

model. This system was modelled by using level set method as mentioned in preceding section. Figure 35 is the geometry of the model,

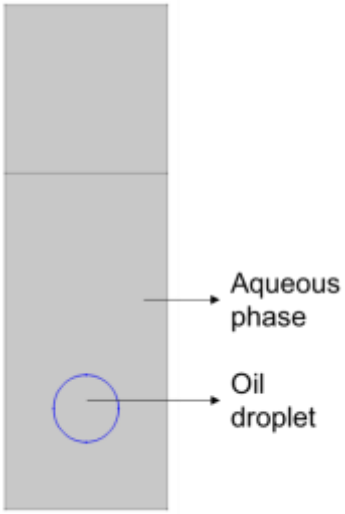

Figure 35 Model geometry of an oil droplet rising in an aqueous phase

A level set function was defined as one for aqueous phase and zero for oil phase, as a result the interface between two phases was tracked by level set function equal to 0.5. Initially the oil droplet is at rest and all solute is concentrated in it. Due to density difference between two phases oil droplet starts rising in an aqueous phase, ultimately it is coalesced with oil phase floating on the top. During this process, solute from the oil phase is extracted in an aqueous phase.

A comparative study of extraction efficiency for a stationary droplet and a mobile droplet was done to study effect of convection on liquid-liquid extraction. A parametric study with varying partition coefficient was done to study the effect of same on liquid-liquid extraction. To obtain solution for this model, Navier-stokes equation and convective diffusion equation are used. Navier-stokes equation which is a momentum balance equation is solved with a continuity equation to obtain a velocity field. The velocity field

obtained from momentum balance is used in convection diffusion equation to account for solute transport and to obtain concentration profile for each phase. These equations are as mentioned in chapter one and chapter four.

For a laminar flow physics, initial velocity and temperature were set to 0 m/s and 298 K respectively. For species transport interface, concentration inside the droplet was set to 100 mols/m^3 and zero in aqueous phase.

Table 4 enlists the boundary conditions for two physics used, laminar flow and transport of diluted species.

Table 4 Boundary conditions

Physics	Boundary condition	Equation
Laminar flow	No slip	$u = 0$
	Volume force	$-g \cdot \rho$
Species transport	Equilibrium condition	$C_1 = kC_2$
	Flux continuity	$D_1 \frac{\partial C_1}{\partial \eta} = D_2 \frac{\partial C_2}{\partial \eta}$
	No flux	$-n \cdot N_i = 0$

For laminar flow interface, a no slip condition was applied at four walls of a channel, a volume force was applied to all the domains. Due to difference in density of oil and aqueous phase, the oil droplet rises.

For a species transport interface, a no flux boundary condition was applied at all four walls, so that no solute is transported in or out of the domain. The most important boundary conditions are applied at the interface between oil droplet and aqueous phase. Following are the two interfacial boundary conditions that are to be satisfied,

A concentration jump is defined by equilibrium assumption,

$$C_1 = KC_2$$

where $C_1$and C_2 are concentration in oil phase and droplet phase respectively, K is partition coefficient.

Second boundary condition applied at the same interface is flux continuity,

$$D_1 \frac{\partial C_1}{\partial \eta} = D_2 \frac{\partial C_2}{\partial \eta}$$

Where D_1 and D_2 are diffusivities of oil and droplet phase respectively.

A concentration jump condition contributes to flux continuity equation, in a way it acts as a constraint. For some value of C_1 and C_2 the equilibrium condition is reached and flux becomes discontinuous and extraction stops. Thus, this equilibrium condition acts as a cap, once reached the solute transport stops.

5.3.2.1 Meshing

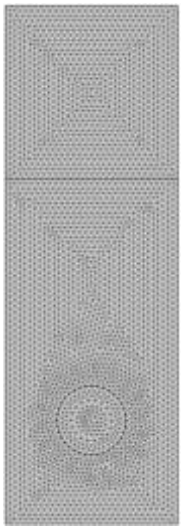

Figure 36 Mesh

All domains are discretized in 7013 elements, free tetrahedral mesh is used. A nonlinear solver is then used to obtain the solution. Results are as discussed in next section.

5.3.2.2 Results and discussion

Figure 37 is a flow field obtained,

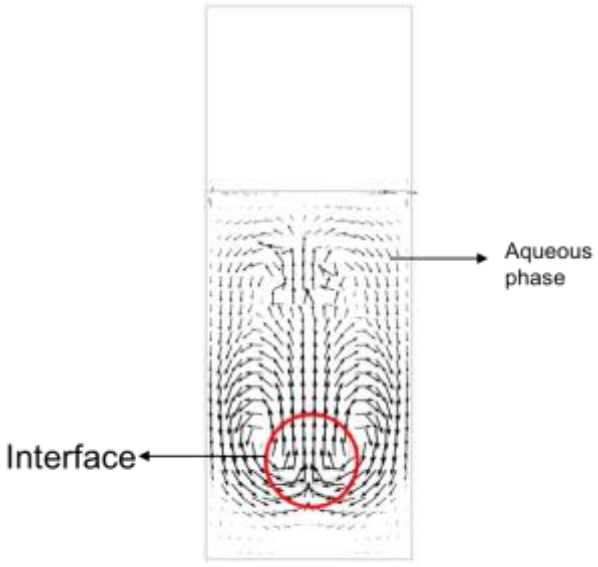

Figure 37 Flow field

As droplet rises, fluid motion is set into both the phases. A recirculating flow can be observed around the droplet.

Figure 38 is a volume fraction plot at various time instances,

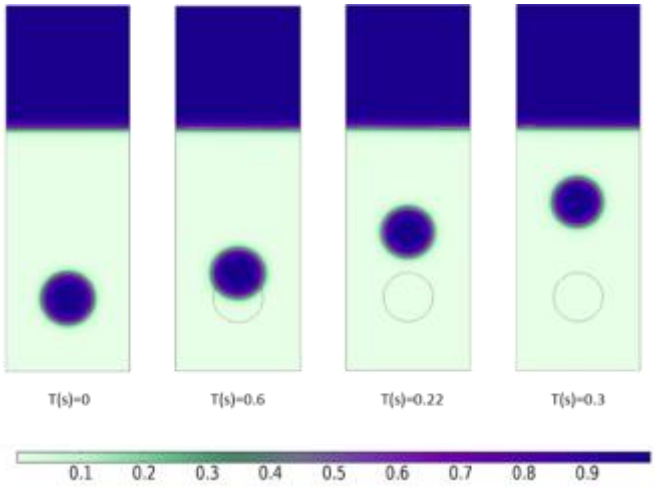

Figure 38 Volume fraction

A volume fraction of one and zero represents oil and aqueous phase respectively, whereas intermediate volume fraction represents the surface phase. Surface phase is an interface which contains molecules of both oil and aqueous phase, also solute transport takes place through this interface. Droplet rising due to density difference is also evident. Figure 39 is the concentration profile,

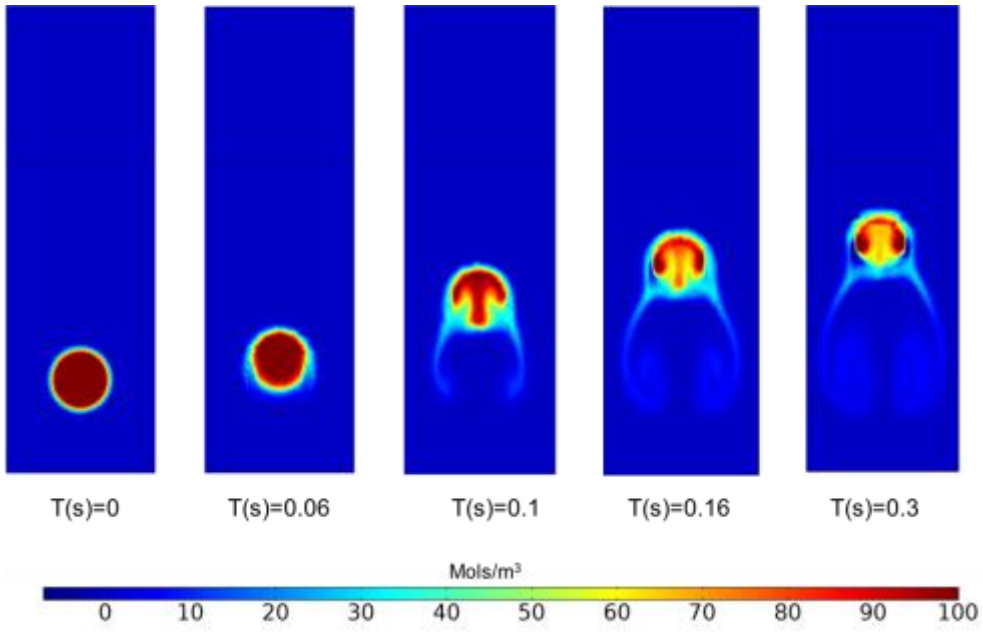

Figure 39 Concentration profile

A plot of concentration at different instants are as shown in Figure 39, decrease in concentration of oil droplet was observed as it was rising. Thus, combined effect of convective flow and diffusion results in extraction. Flow inside the droplet is evident from the flow of solute.

A stationary droplet case was also modelled to study effect of convection on liquid-liquid extraction by comparing it with mobile droplet case, also a parametric study was performed to explore effect of partition coefficient on liquid-liquid extraction. Figure 40 shows result for the same,

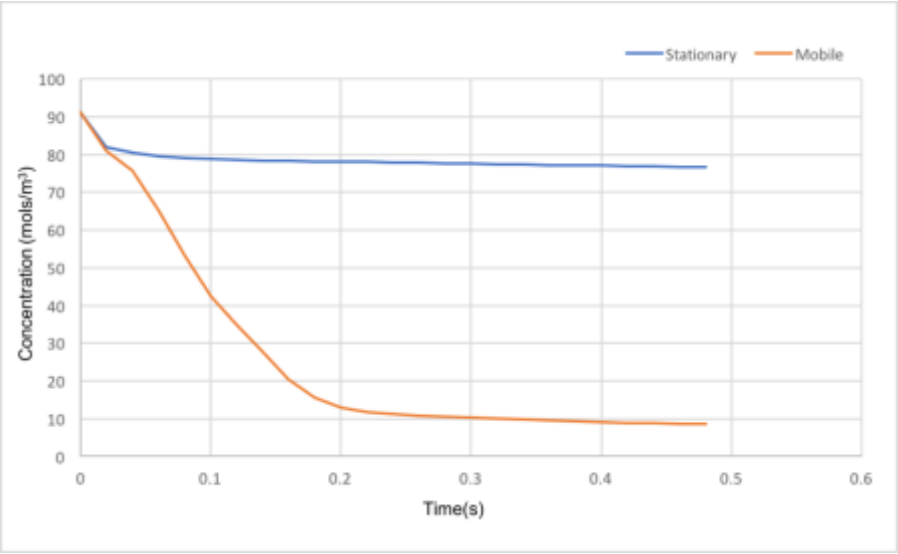

Figure 40 Concentration loss in stationary and mobile droplet

x-axis and y-axis in above plot represents concentration and time respectively. Two data sets are plotted, one for stationary case and other for mobile case. It was observed that the concentration loss in case of mobile droplet was very high when compared with stationary droplet for same time. Thus, convection considerably enhanced the liquid liquid extraction.

For a stationary droplet case, there is no convection inside or outside the droplet, thus the diffusion normal to the iso-concentration line is limiting the mass transport. Moreover, in case of mobile droplet, internal circulation and convection outside the droplet assist in mass transport through interface, furthermore the high surface to volume ration also enhances the mass transport.

It is important to note here that, although mass transfer rate depends on the two-phase hydrodynamics or convection but the interfacial mass transport itself is a purely diffusive phenomenon.

Figure 41 is the plot comparing concentration loss in a droplet for different partition coefficient,

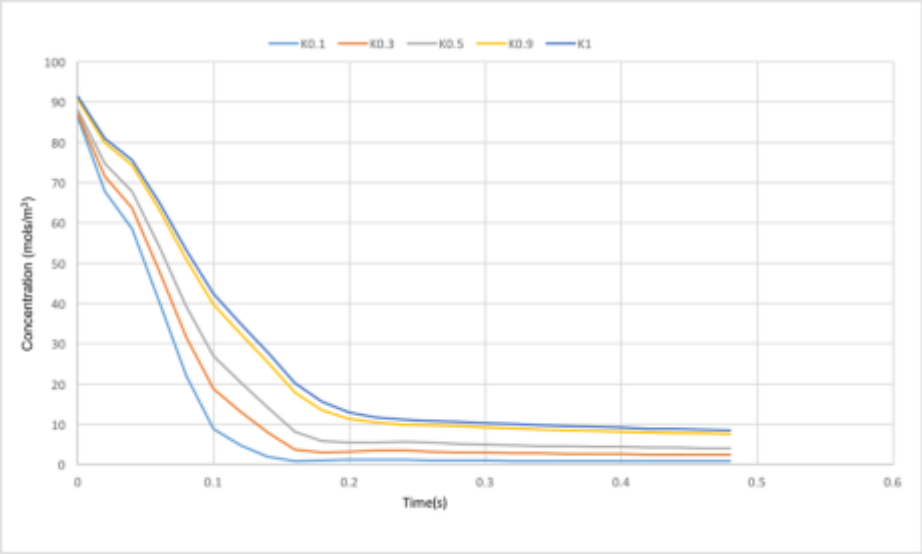

Figure 41 Concentration loss in droplet for different partition coefficient

Partition coefficient determines the equilibrium state of the system, as seen from above figure, equilibrium for each of the different partition coefficient was reached at different concentration. Moreover, extraction efficiency increased with decrease in partition coefficient. As partition coefficient in this case is a ratio of solubility in oil phase to aqueous phase, the resistance to mass transport in aqueous media becomes low for lower value of partition coefficient, thus extraction efficiency increases.

5.3.2.3 Summary

1. Convection greatly enhances liquid-liquid extraction, but mass transport itself takes place by pure diffusion.
2. Due to lower resistance offered to mass transport at lower partition coefficient, mass transfer rate increases with decrease in partition coefficient.

Chapter 6

Enhancement in liquid-liquid extraction by using Marangoni convection

6.1 Introduction

Last chapter concluded that convection enhances liquid liquid extraction. In this chapter, a biphasic fluid system was modelled to study potential of the Marangoni convection to improve interfacial mass transport. A two-phase Multiphysics model was created using a level set method. A set of three physics namely laminar flow, heat transfer and transport of diluted species were coupled and solved to obtain the solution. Following partial differential equations were solved,

Navier stokes equation,

$$\rho\left(\frac{\partial u}{\partial t} + u \cdot \nabla u\right) = -\nabla p + \nabla \cdot (\mu(\nabla u + (\nabla u)^T) + F$$

$$\nabla \cdot (\rho u) = 0$$

Energy equations,

$$\rho C_p \frac{\partial T}{\partial t} + \rho C_p u \cdot \nabla T + \nabla \cdot q = Q + Q_p + Q_{vd}$$
$$q = -K\nabla T$$

Convective diffusion equation,

$$\frac{\partial C}{\partial T} + u \cdot \nabla C = \nabla \cdot (D\nabla C) + R$$

Above equations were solved numerically to obtain solution for velocity field, temperature field and concentration field.

Problem setup, initial conditions and boundary condition are as addressed in the following section.

6.2 Numerical Study

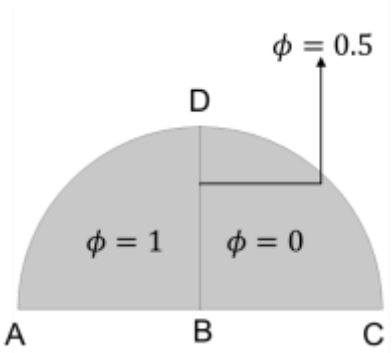

Figure 42 Biphasic fluid system

A biphasic fluid system in Figure 42 includes, water assigned to semicircle ABD and Oil assigned to semicircle CBD. A level set function for semicircle ABD and CBD is defined as one and zero respectively. Initial velocity and temperature were set to 0 and 298 K respectively. Initial concentration of solute was set to 100 mols/m^3 for semicircle CBD and 0 mols/m^3 for semicircle ABC. Boundary conditions are as enlisted in following table,

Table 5 Boundary conditions for laminar flow physics

Boundary	Laminar flow	Heat transfer	Species transport
ABC	No slip	Boundary heat source	No flux
AD	Slip	Heat flux	No flux
CD	Slip	Heat flux	No flux

Flux continuity boundary condition for all three physics is applied at interface BD. A temperature gradient is imposed by heating bottom of two-dimensional droplet which produced a surface tension gradient on the free surface. Thus, a Marangoni convection was generated in both the phases. Effect of the generated Marangoni condition are as discussed in next section.

6.3 Results and discussions

Figure 43 is the volume fraction plot at various instances,

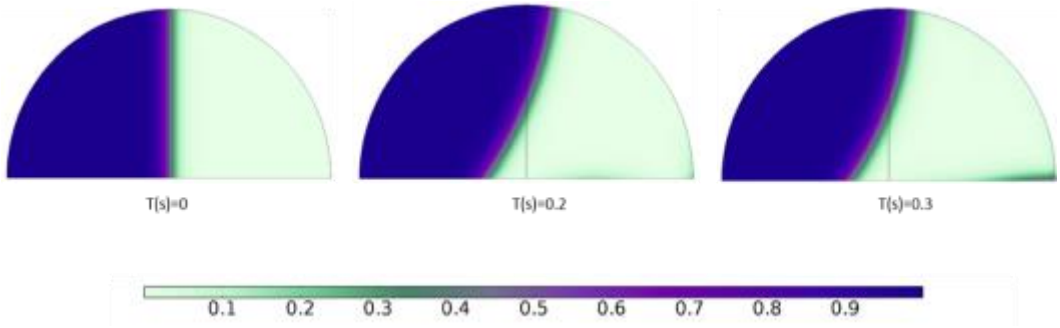

Figure 43 Volume fraction plot

A volume fraction of one represents aqueous phase, whereas volume fraction of zero represents oil phase. Intermediate volume fraction represents a surface face. Surface phase is an interface and it contains molecules of both oil and water.

Figure 44 is the velocity profile,

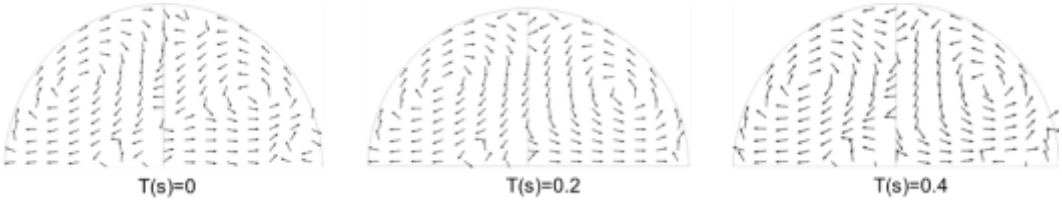

Figure 44 Flow field

Two asymmetric vortices are observed, due to different fluid properties such as density and viscosity. Internal circulation inside the both oil and aqueous phase served two purpose, first one being interface deformation and second one being mixing solute inside both phases. Both phenomena have potential to enhance mass transport through the interface, since hydrodynamics such as convection and surface deformation have proven to enhance liquid-liquid extraction.

Following is the concentration profile,

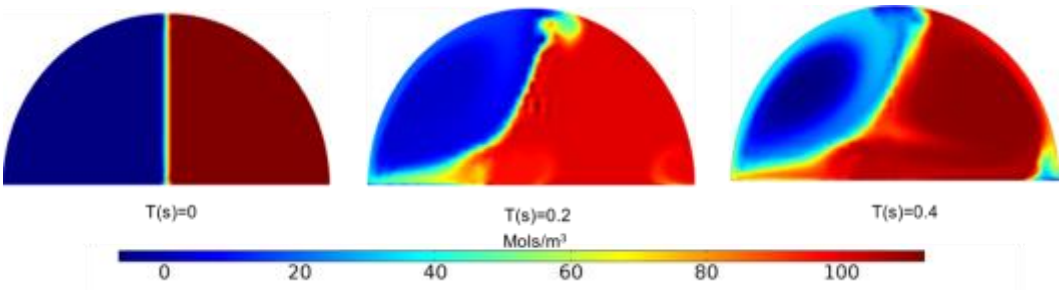

Figure 45 Concentration profile

Figure 45 depicts concentration profile at different instances. Concentration profile at t(s)=0 and t(s)=0.2 represents initial condition and phase initialization respectively. Concentration profile shows effect of Marangoni convection in each phase. A change in concentration was seen in both aqueous and oil phase and mixing of transported species was evident from the rolls formed in each phase.

Thus, linkage between Marangoni convection and mass transport was successfully modelled. Although it was seen that Marangoni convection enhances liquid-liquid extraction but extent of enhancement remains inconclusive.

Chapter 7

Conclusions and future work

From theoretical, experimental and numerical study, it was concluded that:

1. Marangoni flow can be engineered by using various schemes of heating.
2. Accurate control and localization of Marangoni flow can be achieved by changing shape, size and position of heater.
3. Marangoni convection in addition to secondary force can be used for particle separation. Possible secondary force can be dielectrophoretic force or internal convection induced by wetting-dewetting or droplet movement.
4. Marangoni convection have potential application is droplet based chaotic mixing.
5. Convection and interface deformation considerably enhances interfacial mass transport rate, however mass transport occurs due to pure diffusion.
6. Marangoni convection have a potential to enhance liquid liquid extraction, but extent of enhancement remains inconclusive in our study.

In future, an experimental study can be done to measure a potential of Marangoni convection to enhance interfacial mass transport.

Refrences

[1] Berthier, Jean. *Micro-drops and digital microfluidics*. William Andrew, 2012.

[2] Rath, Hans J., ed. *Microgravity Fluid Mechanics: IUTAM Symposium Bremen 1991*. Springer Science & Business Media, 2012.

[3] Tam, Daniel, et al. "Marangoni convection in droplets on superhydrophobic surfaces." *Journal of Fluid Mechanics* 624 (2009): 101-123.

[4] https://www.comsol.com/multiphysics/finite-element-method

[5] https://www.comsol.com/blogs/modeling-marangoni-convection-with-comsol-multiphysics/

[6] https://www.comsol.com/multiphysics/marangoni-effect

[7] Basu, Amar S., and Yogesh B. Gianchandani. "Virtual microfluidic traps, filters, channels and pumps using Marangoni flows." *Journal of Micromechanics and Microengineering* 18.11 (2008): 115031.

[8] Sajeesh, P., and Ashis Kumar Sen. "Particle separation and sorting in microfluidic devices: a review." *Microfluidics and nanofluidics* 17.1 (2014): 1-52.

[9] Di Carlo, Dino. "Inertial microfluidics." *Lab on a Chip* 9.21 (2009): 3038-3046.

[10] B. P. Ho and L. G. Leal, Inertial Migration of Rigid Spheres in Two- Dimensional Unidirectional Flows, J. Fluid Mech., 1974, 65, 365–400.

[11] Di Carlo, Dino, et al. "Continuous inertial focusing, ordering, and separation of particles in microchannels." *Proceedings of the National Academy of Sciences* 104.48 (2007): 18892-18897.

[12] Di Carlo, Dino, et al. "Equilibrium separation and filtration of particles using differential inertial focusing." *Analytical chemistry* 80.6 (2008): 2204-2211.

[13] Nguyen, Nam-Trung. "Mixing in Microscale." *Microfluidic Technologies for Miniaturized Analysis Systems* (2007): 117-155.

[14]http://web.mit.edu/beh.360/www/Fall00/handouts/phase_equil.pdf

[15]https://www.comsol.com/blogs/fat-washing-cocktails-on-an-industrial-scale/

[16] Zimmerman, William BJ. *Process modelling and simulation with finite element methods*. Vol. 1. World Scientific, 2004.

[17] Ganguli, Arijit A., and Eugeny Y. Kenig. "Prediction of Interfacial Mass Transfer in Liquid-Liquid Systems with Moving Interfaces." *10th International Conference on Chemical and Process Engineering, Florence, ITALY*. 2011.

Biographical Information

Viraj Parag Sabane received his bachelor degree from Nagpur University, India in 2014. He joined The University of Texas at Arlington in 2015, where he was a member of Integrated Micro-Nano fluidic laboratory. His research interest includes continuous-flow Microfluidics, Digital Microfluidics, Droplet based Microfluidics.